American Mineralogist, Volume 83, pages 1022–1029, 1998

Structure and dynamics of magnesium in silicate melts: A high-temperature ^{25}Mg NMR study

ANNA M. GEORGE AND JONATHAN F. STEBBINS*

Department of Geological and Environmental Sciences, Stanford University, Stanford, California 94305, U.S.A.

ABSTRACT

^{25}Mg NMR spectra for several silicate and aluminosilicate melts were obtained from 1000–1470 °C. The peaks are initially very broad, but narrow with increasing temperature to near 500 Hz at the highest temperatures. The peak positions for most of the melts do not shift noticeably with temperature in the range studied, except for a sodium magnesium silicate composition that was previously studied by Fiske and Stebbins (1994). This material showed a decrease in frequency of the peak position by about 4 ppm between 1150–1360 °C in both this and the previous study, consistent with an increase in the average size of the site. The chemical shifts vary with composition as well, ranging from 31 ppm for a potassium sodium magnesium silicate melt to 22 ppm for diopside melt ($CaMgSi_2O_6$) at 1400 °C. Compositions with higher field strength cations have lower frequency chemical shifts, which correspond to larger coordination numbers and bond lengths for Mg^{2+}. All of the peak positions obtained fall to slightly higher frequency than the range for sixfold-coordinated Mg in crystals and well below the fourfold-coordinated range, indicating that the Mg is in fivefold to sixfold coordination in the melts. Spin-lattice relaxation times show that measurements are on the high-temperature side of the T_1 minima, and a simple expression for quadrupolar relaxation can be used to obtain correlation times for the motion responsible for the relaxation. The correlation times obtained in this manner are very similar to the correlation time τ_{shear} obtained from viscosity measurements, implying that the Mg motion is strongly coupled to the network motion at these temperatures. Line widths also scale with T_1 in this temperature range, leading to the conclusion that the viscosity is the fundamental limit to observing the ^{25}Mg signal in the melt.

INTRODUCTION

Magnesium is an important component of natural silicate melts, being the fourth most abundant element in the earth after O, Si, and Fe (e.g., Krauskopf and Bird 1995), but its role in the melt structure is not well defined. An understanding of the structure of melts can lead to better models to predict their behavior and could be relevant to geological issues pertaining to igneous rocks such as crystallization, partitioning of elements, diffusion, and viscosity. Although some of these properties are dominated by the network-forming elements (O, Si, Al, etc.), a more complete picture of the material is derived by also considering the local structure and behavior of network-modifying cations like Mg.

Previous studies of the structure of Mg in silicate melts and glasses include molecular dynamics simulations (Matsui et al. 1982; Kubicki and Lasaga 1991; Kubicki and Lasaga 1993; Matsui and Kawamura 1980; Angell et al. 1987), vibrational spectroscopy (Gorbachev et al. 1983; Lisenenkov 1981; Williams et al. 1989; Sykes and Scarfe 1990; Taniguchi and Murase 1987; Kubicki et al. 1992; Hauret et al. 1994), X-ray techniques (Gorbachev et al. 1983; Yin et al. 1983; Waseda and Toguri 1977; Kern et al. 1986; Waseda and Toguri 1990; Taniguchi et al. 1995; Matsubara et al. 1988; Taniguchi et al. 1997; Hanada et al. 1988; Kawazoe et al. 1981), ^{25}Mg NMR spectroscopy (Fiske and Stebbins 1994), and Mg XAFS (Ildefonse et al. 1995; Henderson et al. 1992). Some authors have also made structural inferences from heat capacity measurements (Richet et al. 1993; De Ligny et al. 1996). Most of the above studies discuss one or both of $CaMgSi_2O_6$ (diopside) and $MgSiO_3$ (enstatite) compositions and indicate average bond lengths ranging from 1.88 to 2.18 Å. The coordination numbers reported fall in the range of four to six, though there is little agreement whether Mg occupies a small fourfold-coordinated site or a larger sixfold-coordinated site, as is more common in silicate minerals.

NMR spectroscopy has been used to investigate Mg in silicates only with great difficulty. The sensitivity is low, due to a low natural abundance of the NMR-active isotope (^{25}Mg) and the low resonance frequency. Also, ^{25}Mg is a quadrupolar nuclide, having spin = $5/2$, leading to additional quadrupolar interactions and broadening. Mg sites in silicates are often distorted, leading to broad lines and complicated quadrupolar line shapes that are often difficult to observe.

* E-mail:stebbins@pangea.Stanford.edu

0003–004X/98/0910–1022$05.00

TABLE 1. Compositions and activation energies for spin lattice relaxation of magnesium silicate melts

Name	Composition	Liquidus Temp.(°C)	*Ea*† (kJ/mol)
NaMg2*	$(Na_2O)_{0.28}(MgO)_{0.18}(SiO_2)_{0.54}$	840	119 ± 12
Di	$(MgO)_{0.25}(CaO)_{0.25}(SiO_2)_{0.50}$	1391	158 ± 6
CMAS1	$(MgO)_{0.14}(CaO)_{0.41}(Al_2O_3)_{0.06}(SiO_2)_{0.39}$	~1300	145 ± 10
CMAS2	$(MgO)_{0.21}(CaO)_{0.25}(Al_2O_3)_{0.04}(SiO_2)_{0.5}$	~1345	139 ± 25
KNM	$(Na_2O)_{0.14}(K_2O)_{0.14}(MgO)_{0.18}(SiO_2)_{0.54}$	<960	

* Same composition as in Fiske and Stebbins (1994).
† Derived from 25 Mg spin-lattice relaxation data.

The number of NMR studies of ^{25}Mg in crystalline silicates is limited (Dupree and Smith 1988; MacKenzie and Meinhold 1994; Fiske and Stebbins 1994; MacKenzie and Meinhold 1997). These studies indicate that the ^{25}Mg signal is affected by the local structure around the Mg atoms. The effects of coordination number are particularly apparent: for the limited amount of available data for silicates (not including hydrous silicates), fourfold-coordinated sites fall in the range 49–52 ppm and sixfold-coordinated sites 8–27 ppm (MacKenzie and Meinhold 1994; Fiske and Stebbins 1994). A Mg signal was seen at 55 ppm for a fivefold-coordinated site in grandidierite (MacKenzie and Meinhold 1997), but this material contains as much B as Si. The B could affect the chemical shift, because next-nearest neighbors have been known to affect chemical shifts for other nuclides in silicates (Engelhardt and Michel 1987). Grandidierite also contains a fivefold-coordinated Al site that has a ^{27}Al chemical shift in the range for fourfold-coordinated Al (MacKenzie and Meinhold 1997), possibly for the same reason.

Relationships of chemical shift with coordination number were seen for several other cations in silicates, particularly ^{23}Na, ^{29}Si, ^{27}Al, and ^{6}Li (e.g., Xue and Stebbins 1993; George and Stebbins 1995; Xu and Stebbins 1995; Engelhardt and Michel 1987). In each of these cases, the peak is moved to lower frequency with increasing coordination, as is the case for Mg. This has been explained in terms of a decreasing contribution of the paramagnetic term to the chemical shielding as the bonds become more ionic (George et al. 1997; Engelhardt and Michel 1987). Other structural parameters correlate with coordination number and might correlate with the chemical shift too. For ^{23}Na, trends of decreasing chemical shift with increasing average Na-O bond length and degree of polymerization (NBO/T) also have been observed (Xue and Stebbins 1993; George and Stebbins 1995), and trends with Si-O-Si bond angle have been established for ^{29}Si (Engelhardt and Michel 1987). Insufficient data exists for ^{25}Mg at present to determine whether trends with bond length or angle also hold for Mg. However, the trend with coordination number is consistent among various cations and seems to hold true for fourfold- and sixfold-coordinated Mg.

To our knowledge, there has been only one NMR study of ^{25}Mg in amorphous materials. Fiske and Stebbins (1994) observed Mg in sodium and calcium magnesium silicate melts at high temperatures, and concluded that Mg has an average coordination number of about five in these melts. Furthermore, they observed a shift to lower frequency with increasing temperature in their $(Na_2O)_{0.28}(MgO)_{0.18}(SiO_2)_{0.54}$ composition, which was attributed to a slight increase in the size of the site with temperature. Similar shifts to lower frequency have been observed in silicate melts at high temperature for ^{23}Na (George and Stebbins 1996; Maekawa 1993), as well as for ^{23}Na in borate and germanate melts (George et al. 1997). ^{25}Mg measurements of these materials at lower temperatures were unsuccessful, probably because of the large linewidth expected in the case where motional averaging of the disordered Mg positions is absent in the glass (Fiske and Stebbins 1994). This present study expands the previous work on ^{25}Mg in silicate melts (Fiske and Stebbins 1994) to several new compositions and to higher temperature.

EXPERIMENTAL PROCEDURES

Sample synthesis

Glass samples were prepared using reagent grade Na_2CO_3, SiO_2, Al_2O_3, and $CaCO_3$, as well as 97% enriched ^{25}MgO (Pennwood Chemicals, Inc.). The starting materials were ground together, decarbonated at around 720 °C, melted in a Pt-5%Au crucible at 50–100° above their melting points, and then quenched by putting the crucible in a shallow dish of water. The resulting material was clear glass in all cases, and weight loss measurements indicated that these were close to nominal stoichiometry. Compositions (Table 1) were chosen to have melting temperatures below 1400 °C and relatively low viscosities from 1200–1500 °C. Because of the cost of enriched ^{25}MgO, synthesis batch sizes were limited to the amount needed for one set of measurements: 400–500 mg each.

High *T* NMR spectroscopy

NMR measurements were made using a modified Varian VXR-400S spectrometer, operating at 24.484 MHz for ^{25}Mg. The peak positions were referenced to an external 1M $Mg(NO_3)_2$ solution at room temperature. The pulse length for a 90° radio frequency (rf) tip angle in the liquid was 24 μs at room temperature and increased to about twice that at the higher temperatures (measured on MgO and the glasses) due to the decreased efficiency of the probe at high *T*. The results of 500–1500 pulses were

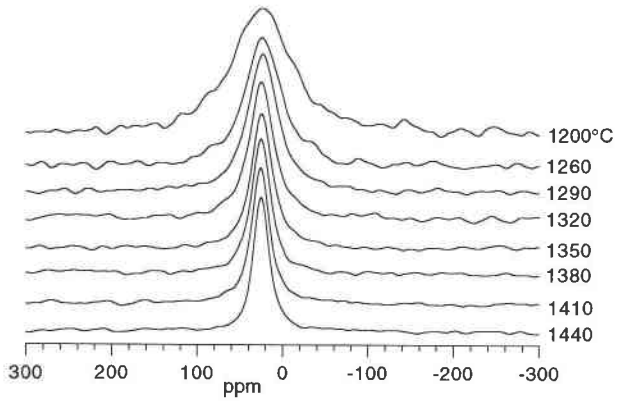

FIGURE 1. Static ^{25}Mg NMR spectra in silicate melt (CMAS1).

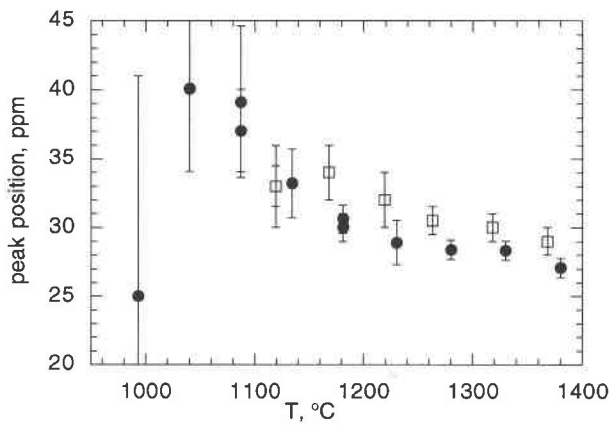

FIGURE 2. ^{25}Mg peak positions in NaMg2 silicate melt. Circles indicate the current data; squares indicate those of Fiske and Stebbins (1994).

averaged for the melt spectra. Relaxation times were measured using an inversion-recovery pulse sequence.

The high-temperature measurements were made using a home-built high-temperature static probe similar to that of Stebbins (1991), modified to use a 7.5 cm, instead of a 5 cm, long-heating element. The samples were contained in a hexagonal boron nitride sample container. The experiments were run under a reducing atmosphere (5%H–95%N) to protect the Mo heating element.

The temperature was calibrated in two separate experiments with a thermocouple encased in alumina placed in the same location as the center of the sample capsule. The error is ±15 °C. Peak positions were corrected for furnace polarity as in Fiske et al. (1994). Both MgO and NaMg2 silicate glass composition (Table 1) were run in the new probe to check for reproducibility of previous data (Fiske et al. 1994; Fiske and Stebbins 1994); the expected results were obtained.

Some reaction with the sample container was observed in the high-temperature experiments: The initially bubble-free glasses were full of bubbles and were very thoroughly adhered to the sample container at the end of the experiment. However, there was no apparent reflection of this reaction in the observed data, as the data obtained on heating were reproducible on cooling.

RESULTS

^{25}Mg signals were only observed at temperatures above 1000 °C; the spectra of CMAS1 are shown in Figure 1. All of the samples showed a dramatic decrease in line width as the temperature increased except for the peak from the KNM composition, which leveled off at a width of about 2000 Hz at 1300 °C and did not narrow further. The peak positions of most of the melts did not appear to change with temperature within the scatter of the data, but the NaMg2 composition of Fiske and Stebbins (1994) showed the same decrease with temperature as observed previously (Fig. 2). This decrease in frequency indicates a slight increase in the size of the site with temperature, although extrapolation of the chemical shift even down to T_g indicates a Mg coordination number around five, which is not too different than that at 1400 °C (see below). The amount of structural change in these materials with temperature in this range does not appear to significantly impact the Mg-coordination number.

By 1400 °C, the lines are narrow enough (except perhaps for KNM) that the peak position is the isotropic chemical shift. By this point, the NMR signals from all five transitions are fully averaged, and the line is narrow and liquid-like. The pulse widths necessary to obtain the maximum signal intensity (90° rf tip angle) for the melts at this temperature are the same as those for crystalline MgO, which is cubic and has a quadrupolar coupling constant of zero, indicating that the transitions are fully averaged in the melt. Comparison of the isotropic chemical shifts in the liquids to those in crystalline materials (Fig. 3) shows that the chemical shifts of the melts at 1400 °C occupy slightly higher frequency than the range for six-fold-coordinated Mg in crystals, but are well below the known fourfold-coordinated range. This fact strongly implies that the coordination number of Mg in these melts at 1400 °C is somewhere between five and six, depending on composition.

Little difference exists between Di and CMAS2 peak positions, indicating that addition of a small amount of Al does not affect the peak position significantly. However, the ^{25}Mg chemical shifts in the melts do appear to vary systematically with type of modifier cation. A comparison of the Di and CMAS1 peak positions at 1400 °C shows that the increased amount of Ca (at the expense of Mg) shifts the peak to higher frequency. The addition of Na also shifts the peak to higher frequency (in NaMg2) and both K and Na further still (in KNM). In general, it seems that the addition of a second modifier cation of lower field strength pushes the peak position to higher frequency, as seen in Figure 3, a plot of chemical shift vs. the average field strength of the modifier cations.

Spin-lattice relaxation times (T_1) were also measured. The fact that the spin-lattice relaxation times increase

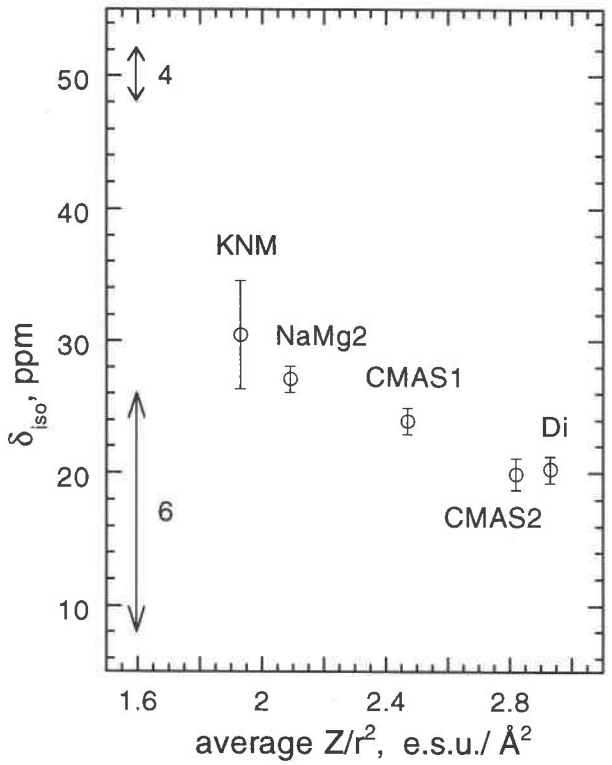

FIGURE 3. ^{25}Mg isotropic chemical shifts in silicate melts near 1400 °C, as a function of average modifier cation field strength [Z/r^2, where Z is the charge and r is the atomic radius in Å taken from Shannon and Prewitt (1969)]. Chemical shift ranges for fourfold- and sixfold-coordinated Mg in crystals at room temperature are shown by arrows.

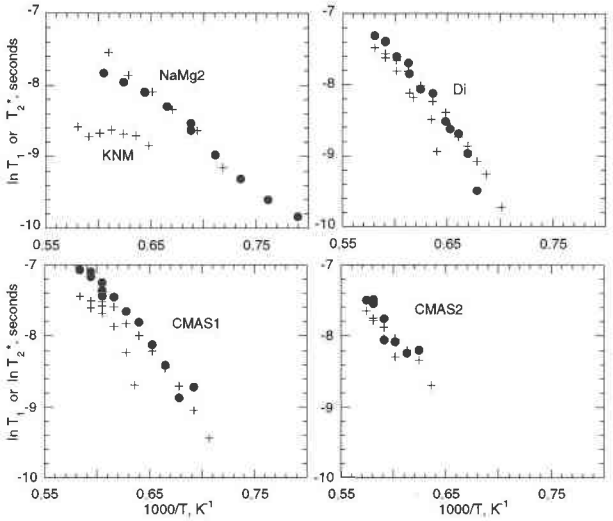

FIGURE 4. Natural logarithms of ^{25}Mg spin-lattice relaxation times in silicate melts plotted against the inverse of absolute temperature. Circles indicate T_1 measure with the inverse-recovery sequence, and crosses are T_2^* obtained from the line widths. Axes on all graphs are the same.

with temperature (Fig. 4) indicates that the observed temperature range is on the high-temperature side of the T_1 minimum, and the frequency of motion causing the quadrupolar relaxation is higher than the Larmor frequency. The activation energies for the motion responsible for relaxation derived from the slopes of the T_1 data range from 119–158 kJ/mol (Table 1). The relaxation times scale with the line widths (FWHM), indicating that the experiments are in a simple regime where the line is "liquid-like" and $T_1 \approx T_2$, where $T_2 = 1/\pi$(FWHM) (Engelhardt and Michel 1987).

Discussion

Peak positions

The idea that the coordination number or size of the site for a cation is correlated with the field strength of other cations present in the material is not unique to Mg. Such relations were shown for other elements as well (e.g., Al^{3+}, Bunker et al. 1991; Ni^{2+}, Galoisy and Calas 1992; and Fe^{3+}, Mysen 1988) and relates to Pauling's second rule. If a higher field strength cation is substituted (higher charge and/or smaller size), the replacement cation takes more of the electron density from the O atoms, leaving less for the Mg, and consequently a necessarily larger average coordination number is necessary to balance the Mg charge. This picture is consistent with the lower frequency chemical shift seen for Mg in the Di and CMAS2 melts, which have higher average field strength modifier cations and might be expected to have larger average Mg sites compared to compositions containing lower field strength cations such as NaMg2 and KNM. Also, a comparison of the compositions of CMAS1 and CMAS2 leads to a prediction of a higher frequency chemical shift for the CMAS1 composition (which differs from CMAS2 and Di in that it contains more Ca and less Mg) because Ca has a lower field strength than Mg, and this indeed is the case. Gorbachev et al. (1983) postulated a change in Mg coordination with composition, with materials containing more Na (lower field strength) having a smaller coordination number than those containing more Mg.

The fact that the Al-containing samples do not have significantly different chemical shifts than similar compositions with no Al (compare Di and CMAS2) is sensible for two reasons. First, the amount of added Al was 6 mol% or less. Second, the other modifier cation present in CMAS2 (Ca) is thought to be more likely than Mg to associate with the Al (Lisenenkov 1981; Sykes and Scarfe 1990), so the Mg site is less likely to be affected.

Much disagreement exists in the literature about the actual coordination number of Mg in silicate glasses and melts. It is possible that some of this disagreement stems from a composition dependence of the size of the average Mg coordination environment, but there remains disagreement even among authors studying the same compositions. Many X-ray studies list average bond lengths that fall near the typical value for sixfold-coordinated sites in crystalline silicates (2.08 Å at room temperature

and 2.12 Å at 1500 °C; Brown et al. 1995), but report coordination numbers near four derived from the area under the Mg-O peak in the radial distribution function (rdf) (Waseda and Toguri 1977; Kern et al. 1986; Taniguchi et al. 1995; Matsubara et al. 1988; Taniguchi et al. 1997; Yin et al. 1983). Some of these authors point out that these long bond lengths in combination with the small coordination numbers would leave the Mg underbonded and that the site is more likely to be a distorted sixfold-coordinated site (Yin et al. 1983; Kern et al. 1986). Molecular dynamics calculations for $MgSiO_3$ and Mg_2SiO_4 melts also predict that Mg resides in a distorted site, with four O atom neighbors near 2 Å and two more near 2.2 Å (Kubicki and Lasaga 1991).

The coordination number obtained from fitting an rdf can be affected by disorder and site distortion and can be model dependent. For a distorted site, the signal from one or more Mg-O pairs could be hidden in the rdf under other contributions, especially since Mg is a relatively weak X-ray scatterer. For this reason, the coordination numbers obtained by fitting the area under the rdf curve are not always accurate (Kubicki and Lasaga 1991; Kern et al. 1986). The bond valence formalism of Brese and O'Keeffe (1991) can also be applied. The bond valence sum (V) around a cation is defined as

$$V = \Sigma_{bonds} \exp[(R - d)/0.37] \quad (1)$$

where R is the bond-valence parameter (1.693 Å for Mg-O bonds) and d the bond distance (Brese and O'Keeffe 1991). This sum should equal the charge on the cation; in the case of Mg, this is two. Using reported bond lengths of 2.04–2.18 Å and a coordination number of four, a bond valence sum of 1.1–1.5 is obtained. Such underbonding is not physically realistic. Thus, the bond lengths seem more consistent with fivefold- to sixfold-coordinated sites.

Henderson et al. (1992) reported bond lengths from Mg-EXAFS ranging from 1.92 Å in a K-Mg leucite glass and 1.98 Å in diopside glass to 2.07 Å for a glass of "basalt" composition. From comparison to typical bond lengths of crystals (Brown et al. 1995), these lengths correspond to coordination numbers of near four for the leucite glass to around five for diopside glass to about six in the basalt composition. The same trend of increasing size of site with field strength is seen in this study, and their probable coordination number of about five for diopside glass is consistent of our estimate of between five and six. Some discrepancy is maybe to be expected, due to possible differences in the glass and melt structures.

The apparent fivefold- to sixfold-coordination environment of Mg in silicate liquids is larger than the fourfold-coordination environment observed for Fe^{2+} (Waychunas et al. 1988, 1989; Jackson et al. 1993) and Ni^{2+} (Farges and Brown 1996; Farges et al. 1995) using XAFS spectroscopy. Because these cations are similar in size to Mg^{2+}, they might be expected to have similar bonding environments in the melt. The reason for the discrepancy is not clear, but it may be related in the differences in bonding between an alkaline earth cation and a transition metal cation. There is also some disagreement about the coordination number of Fe^{2+} and Ni^{2+} in silicate glasses in the literature, e.g., Keppler (1992) asserts distorted octahedral sites, whereas Farges and Brown (1996) and Waychunas et al. (1989) argue that the coordination number is five in glasses.

Farges and Brown (1996) argued that the NMR data of Fiske and Stebbins (1994) could represent fourfold-coordinated Mg if thermal expansion of the bonds was taken into account; however, this calculation was based on estimated bond lengths from the ^{25}Mg NMR. The bond length correlation with ^{25}Mg chemical shifts is somewhat uncertain. If more data are included than used by Fiske and Stebbins (1994), the estimated bond length NaMg2 should be about 2 to 2.06 Å. This observation could represent a coordination number at 1500 °C of up to 5.2, using a similar calculation to that of Farges and Brown (1996). In general, the empirical chemical shift trends with coordination number for cations in silicates are more obvious than those for bond length, and it is more reasonable to trust the coordination numbers than any estimated bond lengths. This is particularly true for Mg, where there is a large difference between the fourfold- and sixfold-coordinated ranges of chemical shifts and a scarcity of data for crystalline silicates upon which to base more subtle trends with bond length or angle. The ^{25}Mg NMR chemical shifts of both Fiske and Stebbins (1994) and this study clearly fall closer to the known range for sixfold-coordinated sites than that seen for fourfold-coordinated sites. It should be noted, however, that the fourfold-coordinated range is based on only two compositions, and is likely to be somewhat broader than indicated in Figure 3.

Relaxation times

A correlation time for the quadrupolar fluctuations causing relaxation can be calculated from spin-lattice relaxation times on the high-temperature side of the T_1 minimum using the relation for quadrupolar relaxation in a liquid (Abragam 1961)

$$\frac{1}{T_1} = \frac{3\pi^2}{10} \frac{2I + 3}{I^2(2I - 1)} \left(\frac{e^2qQ}{h}\right)^2 \left(1 + \frac{\eta^2}{3}\right) \tau_c. \quad (2)$$

In this expression, e^2qQ/h is the quadrupolar coupling constant, η the quadrupolar asymmetry parameter, I the nuclear spin, T_1 the NMR spin-lattice relaxation time, and τ_c the correlation time. For our melts, τ_c can be estimated by assuming QCC = 4.5 MHz and $\eta = 0$. The asymmetry parameter η does not have a large impact on the final value, and the QCC value was chosen because it was similar to that observed in crystals (Fiske and Stebbins 1994).

The correlation times in Figure 5 can be compared to those derived from viscosity data to determine whether or not the Mg motion is coupled to that of the network at these temperatures. The shear relaxation time τ_{shear} is given by

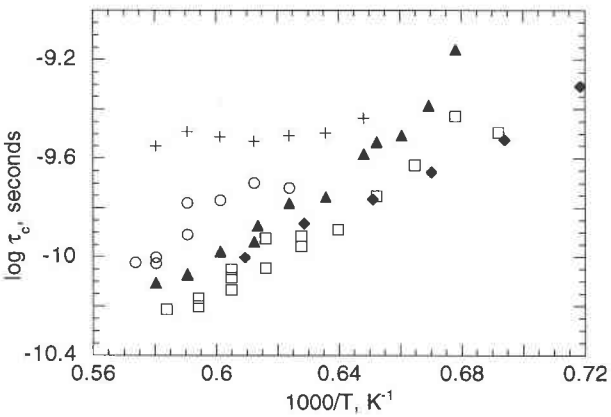

FIGURE 5. Log_{10} of correlation times calculated from NMR T_1 data plotted against the inverse of absolute temperature. Circles = CMAS2; triangles = Di; diamonds = NaMg2; squares = CMAS1; and crosses = KNM.

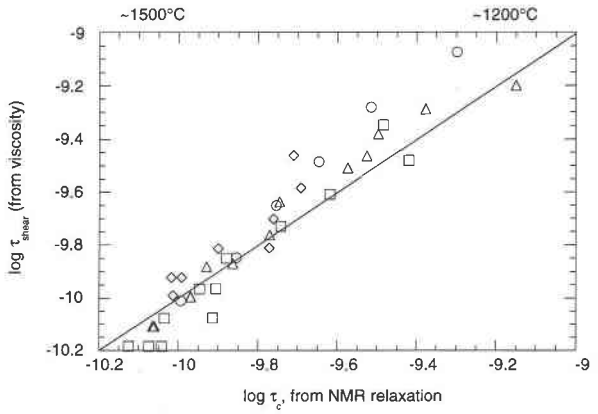

FIGURE 6. Comparison of $Log_{10}\tau_{shear}$, calculated from viscosity data to τ_c derived from ^{25}Mg NMR relaxation times in silicate melts. Circles = NaMg2; squares = CMAS1; triangles = Di; and diamonds = CMAS2. The line indicates where $\tau_{shear} = \tau_c$. Viscosity data from Bansal and Doremus (1986) and Ryan and Blevins (1987). Temperature labels indicate approximate ranges of these compositions for the correlation times shown.

$$\tau_{shear} = \frac{\eta}{G_\infty} \quad (3)$$

where η is the viscosity and G_∞ the infinite frequency shear modulus, commonly taken to be 10 GPa (Stebbins 1995). The τ_{shear} values thus calculated are very close to the τ_c calculated from the ^{25}Mg T_1 data (Fig. 6), indicating that the frequency of Mg motion is similar to that of the network at these temperatures in the melts.

This coupling to the network for Mg contrasts with the behavior of Na, which is coupled to the network at high temperatures, but progressively decouples as the temperature decreases. Data for both elements in different compositions can be compared by plotting τ vs. a temperature scaled by the glass transition temperature (i.e., vs. Tg/T). Comparison of ^{23}Na in $Na_2Si_3O_7$ (Sen et al. 1996) to ^{25}Mg in Di in Figure 7 shows that Mg remains coupled to the network motion at much lower temperatures than the point at which Na begins to decouple. This reflects the stronger bonding to the network that magnesium experiences compared to an alkali ion. Similar comparisons can be made for the other compositions in this study.

Because the relaxation times scale with the viscosity in this temperature region, and the line widths are controlled by T_1, the ^{25}Mg line width is entirely governed by the viscosity of the liquid. This severely limits observation of a Mg signal to compositions whose viscosities are relatively low below 1500 °C and adds to the difficulty of the experiment. This correlation of the line width with viscosity is likely to be the reason that the ^{25}Mg lines are too broad to observe in glasses at lower temperatures.

We were unable to locate viscosity data for the KNM composition to compare to the almost invariant τ_c from ^{25}Mg relaxation times. It is possible that this composition shows relatively "fragile" dynamical behavior (Angell 1991), with a viscosity curve that changes only slowly with temperature in this region. Another alternative is that we are actually very close to the T_1 minimum, where T_1 is difficult to measure and the T_1 curve flattens out. If this were the case, the T_1 minimum for this composition would be at a much higher temperature than that for the pure sodium composition (which is at lower temperature than we could observe) and would give evidence for the large K ions hindering Mg motion. A final possibility is that the NMR relaxation correlation times are beginning to decouple from the shear correlation times in this com-

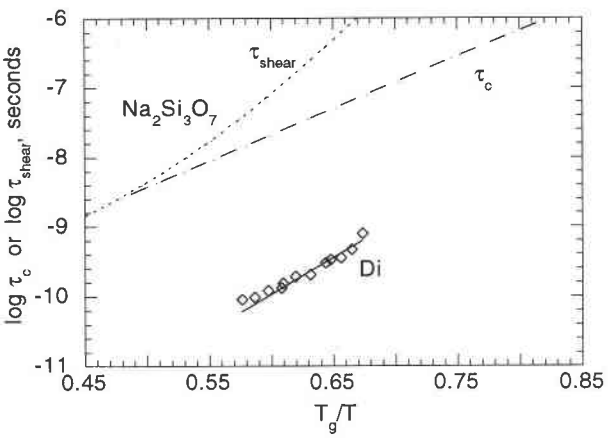

FIGURE 7. Comparison of the extent of modifier cation coupling to the silicate network for Mg^{2+} and Na^+ in silicate melts. The dotted line shows τ_{shear}, calculated from the viscosity data for $Na_2Si_3O_7$ melt, and the dashed line shows correlation times derived from ^{23}Na NMR data for that same composition [23Na data from George and Stebbins (1996) and Sen et al. (1996)]. The solid line shows τ_{shear} calculated from the viscosity of diopside melt, and the diamonds are the correlation times derived from ^{25}Mg T_1 data. Data are plotted against the inverse of absolute temperature, multiplied by the glass transition temperature T_g, to scale dynamics properly.

position. In the similar NaMg2 composition, it is possible that the NMR relaxation correlation times are also beginning to decouple from the shear correlation times at lower temperatures (Fig. 6), but the uncertainties in these points are too large to say this with any confidence.

Acknowledgments

This work was funded under NSF grant no. EAR-9506393. The authors thank S. Sen for useful comments regarding the comparison of Na and Mg relaxation data, and G.E. Brown Jr., G.A. Waychunas, D. Massiot, and an anonymous reviewer for reviews of the manuscript.

References cited

Abragam, A. (1961) Principles of Nuclear Magnetism, 599 p. Clarendon Press, Oxford.

Angell, C.A. (1991) Relaxation in liquids, polymers, and plastic crystals: Strong/fragile patterns and problems. Journal of the American Chemical Society, 131–133, 13–31.

Angell, C.A., Cheeseman, P.A., and Kadiyala, R.R. (1987) Diffusivity and thermodynamic properties of diopside and jadeite melts by computer simulation studies. Chemical Geology, 62, 83–92.

Bansal, N.P. and Doremus, R.H. (1986) Handbook of Glass Properties, 680 p. Academic Press, Orlando.

Brese, N.E. and O'Keeffe, M. (1991) Bond-valence parameters for solids. Acta Crystallographica, B47, 192–197.

Brown, G.E. Jr., Farges, F. and Calas, G. (1995) X-ray scattering and X-ray spectroscopy studies of silicate melts. In Mineralogical Society of America Reviews in Mineralogy, 32, 317–401.

Bunker, B.C., Kirkpatrick, R.J., Brow, R.K., Turner, G.L., and Nelson, C. (1991) Local structure of alkaline-earth boroaluminate crystals and glasses: II, ^{11}B and ^{27}Al MAS NMR spectroscopy of alkaline-earth boroaluminate glasses. Journal of the American Ceramic Society, 74, 1430–1438.

de Ligny, D., Westrum, E.F. Jr., and Richet, P. (1996) Entropy of calcium and magnesium aluminosilicate glasses. Chemical Geology, 128, 113–128.

Dupree, R. and Smith, M.E. (1988) Solid-state magnesium-25 NMR spectroscopy. Journal of the Chemical Society, Chemical Communications, 1483–1485.

Engelhardt, G. and Michel, D. (1987) High-Resolution Solid-State NMR of Silicates and Zeolites, 485p. Wiley, New York.

Farges, F. and Brown, G.E. Jr. (1996) An empirical model for the anharmonic analysis of high-temperature XAFS spectra of oxide compounds with applications to the coordination environment of Ni in NiO, γ-Ni_2SiO_4, and Ni-bearing Na-disilicate glass and melt. Chemical Geology, 128, 93–106.

Farges, F., Brown, G.E. Jr., Calas, G., Galoisy, L., and Waychunas, G.A. (1995) Local structure change around 2 wt % of Ni in a $Na_2Si_2O_5$ melt. Physica B, 208–209, 381–382.

Fiske, P.S. and Stebbins, J.F. (1994) The structural role of Mg in silicate liquids: A high-temperature ^{25}Mg, ^{23}Na, and ^{29}Si NMR study. American Mineralogist, 79, 848–861.

Fiske, P.S., Stebbins, J.F., and Farnan, I. (1994) Bonding and dynamical phenomena in MgO: A high-temperature ^{17}O and ^{25}Mg NMR study. Physics and Chemistry of Minerals, 20, 587–593.

Galoisy, L. and Calas, G. (1992) Network-forming Ni in silicate glasses. American Mineralogist, 77, 677–680.

George, A.M. and Stebbins, J.F. (1995) High-temperature ^{23}Na MAS NMR data for albite: Comparison to chemical-shift models. American Mineralogist, 80, 878–884.

———(1996) Dynamics of Na in sodium aluminosilicate glasses and liquids. Physics and Chemistry of Minerals, 23, 526–534.

George, A.M., Sen, S., and Stebbins, J.F. (1997) ^{23}Na chemical shifts and local structure in crystalline, glassy, and molten sodium borates and germanates. Solid State NMR, 10, 9–18.

Gorbachev, V.V., Bystrikov, A.S., Vasil'ev, S.K., and Bogomolova, L.V. (1983) An X-ray spectra study of the state of magnesium ions in sodium magnesium and sodium calcium magnesium silicate glasses. Soviet Journal of Glass Physics and Chemistry, 9, 447–452.

Hanada, T., Soga, N., and Tachibana, T. (1988) Coordination state of magnesium ions in rf-puttered amorphous films in the system MgO-SiO_2. Journal of Non-Crystalline Solids, 105, 39–44.

Hauret, G., Vaills, Y., Luspin, Y., Gervais, F., and Cote, B. (1994) Similarities in the behavior of magnesium and calcium in silicate glasses. Journal of Non-Crystalline Solids, 170, 175–181.

Henderson, C.M.B., Charnock, J.M., Van der Laan, G., and Schreyer, W. (1992) X-ray absorption spectroscopy of Mg in minerals and glasses. Synchrotron Radiation: Appendix to Daresbury Annual Report 1991/1992, 77.

Ildefonse, P., Calas, G., Flank, A.M., and Lagarde, P. (1995) Low Z elements (Mg, Al, and Si) K-edge X-ray absorption spectroscopy in minerals and disordered systems. Nuclear Instruments and Methods in Physics Research B, 97, 172–175.

Jackson, W.E., Waychunas, G.A., Brown, G.E. Jr., Mustre de Leon, J., Conradson, S., and Combes, J.-M. (1993) High-temperature XAS study of Fe_2SiO_4: evidence for reduced coordination of ferrous iron in the liquid. Science, 262, 229–233.

Kawazoe, H., Kokumai, H., Kanazawa, T., and Gohshi, Y. (1981) Coordination of Mg^{2+} in oxide glasses determined by X-ray emission spectroscopy. Journal of the Physics and Chemistry of Solids, 42, 579–581.

Kern, E.M., Chernyavskii, I.Y., Zyat'kova, L.R., and Vatolin, N.A. (1986) X-ray study of the structure of a magnesium melt. Soviet Journal of Glass Physics and Chemistry, 12, 9–14.

Keppler, H. (1992) Crystal field spectra and geochemistry of transition metal ions in silicate melts and glasses. American Mineralogist, 77, 62–75.

Krauskopf, K.B. and Bird, D.K. (1995) Introduction to Geochemistry, 647 p. McGraw-Hill, New York.

Kubicki, J.D. and Lasaga, A.C. (1991) Molecular dynamics simulation of pressure and temperature effects on $MgSiO_3$ and Mg_2SiO_4 melts and glasses. Physics and Chemistry of Minerals, 17, 661–673.

———(1993) Molecular dynamics simulations of interdiffusion in $MgSiO_3$-Mg_2SiO_4 melts. Physics and Chemistry of Minerals, 20, 255–262.

Kubicki, J.D., Hemley, R.J., and Hofmeister, A.M. (1992) Raman and infrared study of pressure-induced structural changes in $MgSiO_3$, $CaMgSi_2O_6$, and $CaSiO_3$ glasses. American Mineralogist, 77, 258–269.

Lisenenkov, A.A. (1981) Distribution of calcium and magnesium cations between silicate and aluminosilicate anions. Soviet Journal of Glass Physics and Chemistry, 23, 547–550.

MacKenzie, K.J.D. and Meinhold, R.H. (1994) ^{25}Mg nuclear magnetic resonance spectroscopy of minerals and related inorganics: A survey study. American Mineralogist, 79, 250–260.

———(1997) MAS NMR study of pentacoordinated magnesium in grandidierite. American Mineralogist, 82, 479–482.

Maekawa, H. (1993) NMR studies of the structure and dynamics of silicate melts, Ph. D. thesis, Hokkaido University, Sapporo, Japan.

Matsubara, E., Kawazoe, T., Waseda, Y., Ashizuka, M., and Ishida, E. (1988) Oxygen coordination of magnesium and calcium in binary magnesia and calcia metaphosphate glasses. Journal of Materials Science, 23, 547–550.

Matsui, Y. and Kawamura, K. (1980) Instantaneous structure of an $MgSiO_3$ melt simulated by molecular dynamics. Nature, 285, 648–649.

Matsui, Y., Kawamura, K., and Syono, Y. (1982) Molecular dynamics calculations applied to silicate systems: Molten and vitreous $MgSiO_3$ and $MgSiO_4$ under low and high pressure. In F. Marumo, Ed., High Pressure Research in Geophysics: Advances in Earth and Planetary Sciences, 12 p. 511–524, Reidel, Boston.

Mysen, B.O. (1988) Structure and Properties of Silicate Melts, 354 p. Elsevier, Amsterdam.

Richet, P., Robie, R.A., and Hemingway, B.S. (1993) Entropy and structure of silicate glasses and melts. Geochimica et Cosmochimica Acta, 57, 2751–2766.

Ryan, M.P. and Blevins, J.Y.K. (1987) The viscosity of synthetic and natural silicate melts and glasses at high temperatures and 1 bar (10^5 Pascals) pressure and higher pressure. USGS Survey Bulletin no. 1764.

Sen, S., George, A.M., and Stebbins, J.F. (1996) Ionic conduction and

mixed cation effect in silicate glasses and liquids: ^{23}Na and ^{7}Li NMR spin-lattice relaxation and a multiple-barrier model of percolation. Journal of Non-Crystalline Solids, 197, 53–64.

Shannon, R.D. and Prewitt, C.T. (1969) Effective ionic radii in oxides and fluorides. Acta Crystallographica, B25, 925–945.

Stebbins, J.F. (1991) Nuclear magnetic resonance at high temperature. Chemical Reviews, 91, 1353–1373.

———(1995) Dynamics and structure of silicate and oxide melts: Nuclear magnetic resonance studies. In Mineralogical Society of America Reviews in Mineralogy, 32, 191–239.

Sykes, D. and Scarfe, C.M. (1990) Melt structure in the system nepheline-diopside. Journal of Geophysical Research, 95 (B10), 15745–15749.

Taniguchi, H. and Murase, T. (1987) Some physical properties and melt structures in the system diopside-anorthite. Journal of Volcanology and Geothermal Research, 34, 51–64.

Taniguchi, T., Okuno, M., and Matsumoto, T. (1995) The structural studies of $CaMgSi_2O_6$, $CaCoSi_2O_6$ and $CaNiSi_2O_6$. Mineralogical Journal, 17, 231–244.

———(1997) X-ray diffraction and EXAFS studies of silicate glasses containing Mg, Ca, and Ba atoms. Journal of Non-Crystalline Solids, 211, 56–63.

Waseda, Y. and Toguri, J.M. (1977) The structure of molten binary silicate systems $CaO\text{-}SiO_2$ and $MgO\text{-}SiO_2$. Metallurgical Transactions, 8B, 563–568.

———(1990) Structure of silicate melts determined by X-ray diffraction. In F. Marumo, Ed., Dynamic Processes of Material Transport and Transformation in the Earth's Interior, p. 37–51. Terra Scientific Publishing Company, Tokyo.

Waychunas, G.A., Brown, G.E. Jr., Jackson, W.E., and Ponader, C.W. (1989) In situ high temperature X-ray absorption study of iron in alkalisilicate melts and glasses. Physica B, 158, 67–68.

Waychunas, G.A., Brown, G.E. Jr., Ponader, C.W., and Jackson, W.E. (1988) Evidence from X-ray absorption for network forming Fe^{2+} in molten silicates. Nature, 332, 251–253.

Williams, Q., McMillan, P., and Cooney, T.F. (1989) Vibrational spectra of olivine composition glasses: the Mg-Mn join. Physics and Chemistry of Minerals, 16, 352–359.

Xu, Z. and Stebbins, J.F. (1995) ^{6}Li nuclear magnetic resonance chemical shifts, coordination number and relaxation in crystalline and glassy silicates. Solid State NMR, 5, 103–112.

Xue, X. and Stebbins, J.F. (1993) ^{23}Na NMR chemical shifts and local Na coordination environments in silicate crystals, melts, and glasses. Physics and Chemistry of Minerals, 20, 297–307.

Yin, C.D., Okuno, M., Morikawa, H., and Marumo, F. (1983) Structure analysis of $MgSiO_3$ glass. Journal of Non-Crystalline Solids, 55, 131–141.

Manuscript received December 23, 1997
Manuscript accepted April 5, 1998
Paper handled by Hans Keppler